

2.2 Ocean Drilling Perspectives on Meteorite Impacts

Christopher Lowery*¹, Joanna V. Morgan², Sean P.S. Gulick¹, Timothy J. Bralower³, Gail L. Christeson¹, Exp. 364 Scientists⁴

¹University of Texas Institute for Geophysics, Jackson School of Geosciences, Austin, USA

²Department of Earth Science and Engineering, Imperial College, London, UK

³Department of Geosciences, Pennsylvania State University, University Park, USA

⁴see list of science party members at the end

*corresponding author: cmlowery@utexas.edu; Research Associate, University of Texas Institute for Geophysics, JJ Pickle Research Campus 10100 Burnet Rd., Austin, TX, 78758
ORCID: <https://orcid.org/0000-0002-0101-4397>

Abstract

Extraterrestrial impacts are a ubiquitous process in the solar system, reshaping the surface of rocky bodies of all sizes. On early Earth, impact structures may have been a nursery for the evolution of life. More recently, a large meteorite impact caused the end-Cretaceous mass extinction, causing the extinction of 75% of species known from the fossil, including non-avian dinosaurs, and clearing the way for the dominance of mammals and eventual evolution of humans. Understanding the fundamental processes associated with impact events is critical to understanding the history of life on Earth, and the potential for life in our solar system and beyond.

Scientific ocean drilling has generated a large amount of unique data on impact processes. With the constant subduction and creation of oceanic crust, the Chicxulub impact is the single largest and most significant impact event that can be studied by sampling modern ocean basins. Marine sediment cores have been instrumental in quantifying the environmental, climatological, and biological effects of that impact. Drilling in the Chicxulub Crater has significantly advanced our understanding of fundamental impact processes, notably the formation of peak rings in large impact craters, but also raised new questions waiting to be addressed with further drilling. Within the crater, the nature and thickness of the melt sheet in the central basin is unknown, and an expanded Paleocene hemi-pelagic section would provide insights to both the recovery of life and the climatic changes after the impact. Globally, new

32 cores in the Pacific could directly sample the downrange ejecta of this northeast-southwest
33 trending impact.

34 Extraterrestrial impacts have been controversially suggested as primary drivers for many
35 important paleoclimatic and environmental events throughout Earth History. However, marine
36 sediment archives and geochemical proxies (e.g., Osmium isotopes) provide a long-term archive
37 of major impact events in recent Earth history and show that, other than the end-Cretaceous,
38 significant environmental changes do not appear to be driven by impacts.

39

40 **Keywords:** Ocean Drilling, Impact Events, Cretaceous-Paleogene, Chicxulub Crater,
41 Chesapeake Bay Crater, Popigai Crater, Mass Extinction

42

43 **1 Introduction**

44 Large meteorite impacts have had a significant influence on Earth history, possibly
45 driving the early evolution of life (e.g., Kring, 2000, 2003; Nisbet and Sleep, 2001) and the
46 composition of the oceans and atmosphere (e.g., Kasting 1993). They also have the potential to
47 completely reshape the biosphere (e.g., Smit and Hertogen, 1980; Alvarez et al., 1980). The
48 Cretaceous-Paleogene (K-Pg) mass extinction, almost certainly caused by the impact of a
49 meteorite on the Yucatán carbonate platform of Mexico 66 Ma, is the most recent major mass
50 extinction of the so-called Big Five (e.g., Raup and Sepkoski, 1982). It ended the dominance of
51 non-avian dinosaurs, marine reptiles, and ammonites, and set the stage for the Cenozoic
52 dominance of mammals that eventually led to the evolution of humans (Schulte et al., 2010;
53 Meredith et al., 2011). The environmental effects of the Chicxulub impact and the resulting mass
54 extinction occurred over a geologically brief period of time (with the major climatic changes
55 lasting years to decades, e.g., Brugger et al., 2017), and the subsequent recovery of life provides
56 an important partial analog for the recovery of biodiversity following geologically rapid
57 anthropogenic extinction due to climate change, acidification, and eutrophication.

58 The K-Pg impact hypothesis was controversial when first proposed (Smit and Hertogen,
59 1980; Alvarez et al., 1980), but careful correlation of impact material from K-Pg boundary

60 sections led to its gradual acceptance (e.g., Schulte et al., 2010). The discovery of the Chicxulub
61 Crater (Penfield and Carmargo, 1981; Hildebrand et al., 1991) and its clear genetic relationship
62 with K-Pg boundary ejecta provided compelling evidence for this hypothesis. Scientific ocean
63 drilling has been instrumental in discovering widespread physical, chemical, and biological
64 supporting evidence, and in documenting the global environmental and biotic effects of the
65 impact (e.g., see summary in Schulte et al., 2010). Drilling by IODP Expedition 364 into the
66 Chicxulub Crater itself has yielded valuable insights into the mechanisms of large impact crater
67 formation and the recovery of life (Morgan et al., 2016; Morgan et al., 2017; Artemieva et al.,
68 2017; Christeson et al., 2018; Lowery et al., 2018; Riller et al., 2018).

69 Although the K-Pg is the only mass extinction that is widely (though not universally)
70 accepted to have been caused by an extraterrestrial collision, impacts have been suggested at one
71 point or another as drivers for every major Phanerozoic extinction event (e.g., Rampino and
72 Stothers, 1984) and many other major climate events (e.g., Kennett et al., 2009; Schaller et al.,
73 2016). The discovery of an iridium layer at the K-Pg boundary as the key signature of
74 extraterrestrial material (Alvarez et al., 1980) spurred the search for other impact horizons
75 through the careful examination of many other geologically significant intervals, and so far no
76 other geologic event or transition has met all the criteria to indicate causation by an impact (e.g.,
77 the presence of Ir and other platinum group elements in chondritic proportions; tektites; shock-
78 metamorphic effects in rocks and minerals; perturbation of marine Os isotopes; and, ideally, an
79 impact crater), although many periods would meet at least one of these (e.g., Sato et al., 2013;
80 Schaller et al., 2016; Schaller and Fung, 2018) and the search for impact evidence continues.

81 For the last 50 years the Deep Sea Drilling Project (DSDP), Ocean Drilling Program
82 (ODP), Integrated Ocean Drilling Program, and International Ocean Discovery Program (IODP)
83 have provided a unique and irreplaceable perspective on the history of the Earth. IODP and its
84 sister organization the International Continental scientific Drilling Program (ICDP) produce
85 insights into impact cratering processes and effects of different magnitude events, as well as
86 target rocks, on the climate and biosphere, providing an exceptional record of processes that are
87 ubiquitous across the solar system (and, presumably, beyond). This contribution focuses on
88 ocean drilling perspectives on meteorite impacts; important contributions from onshore drilling
89 by ICDP into the Chesapeake Bay, Chicxulub, Lake Bosumtwi, and Lake El'gygytgyn impact

90 craters are summarized by Gohn et al. (2008), Urrutia-Fucugauchi et al. (2004), Koeberl et al.
91 (2007), and Melles et al. (2012).

92 Here we examine the contributions of scientific ocean drilling into our understanding of
93 impact events, from detailed records of extinction and chemical and physical perturbation in the
94 marine realm to the mechanisms by which rocks are deformed to create peak rings in impact
95 craters. The exciting results of recent drilling in the Chicxulub crater raise new questions, and
96 suggest promising new challenges and avenues of investigation of deep sea records of impact
97 events that can only be undertaken by a program like IODP.

98 **2 Marine Record of Impacts**

99 Scientific ocean drilling excels at providing raw material to generate high-resolution
100 composite records of geochemical changes in the ocean through time. One of these proxies is the
101 isotopic ratio of osmium ($^{187}\text{Os}/^{188}\text{Os}$) in sea water, as reflected in marine sediments. Os isotopes
102 in ocean water are the result of secular changes in the amount of mantle-derived (depleted in
103 ^{187}Os) and crustal materials (enriched in ^{187}Os) (Pegram et al., 1992). Changes in the $^{187}\text{Os}/^{188}\text{Os}$
104 of marine sediments over time can be used as a proxy for flood basalt volcanism (e.g., Turgeon
105 and Creaser, 2008), weathering flux (Ravizza et al., 2001), ocean basin isolation (e.g., Poirier
106 and Hillaire-Marcel, 2009), and, importantly for our purposes, the detection of impact events
107 (Turekian, 1982; Peucker-Ehrenbrink and Ravizza, 2000, 2012; Paquay et al., 2008). Chondritic
108 meteors have an Os isotopic ratio similar to that of the mantle, and extraterrestrial impacts result
109 in a strong, rapid excursion to unradiogenic (i.e., closer to 0) marine $^{187}\text{Os}/^{188}\text{Os}$ ratios (Luck and
110 Turekian, 1983; Koeberl, 1998; Reimold et al., 2014) (Figure 1). The only two such excursions
111 in the Cenozoic are Chicxulub (Figure 1B) and the late Eocene (~35 Ma; Poag et al., 1994;
112 Bottomley et al., 1997) dual impacts at Chesapeake Bay on the North American Atlantic coastal
113 plain and Popigai in Siberia (Fig 1C) (Robinson et al., 2009; Peucker-Ehrenbrink and Ravizza,
114 2012). Other major climate events which have been proposed to be associated with impacts, like
115 the Paleocene-Eocene Thermal Maximum (PETM; e.g., Schaller et al., 2016) (Figure 1D), and
116 the Younger Dryas (e.g., Kennett et al., 2009) (Figure 1F) are not associated with any clear
117 excursion toward unradiogenic values, despite relatively high sample resolution (e.g., Paquay et
118 al., 2009). Indeed, the PETM shows a positive excursion of Os isotope values associated with
119 enhanced weathering during the event (Ravizza et al., 2001). Of course, such an Os isotope

120 excursion would only be expected from chondritic impactors, and even then the scale of the
121 impact is not necessarily reflected in the size of the Os excursion (Morgan, 2008).

122 Ocean drilling has directly sampled ejecta from several Cenozoic craters. Tektites from
123 the late Eocene Chesapeake Bay and Popigai impacts were recovered from DSDP and ODP Sites
124 94 (Gulf of Mexico), 149 (Caribbean), and 612, 903, 904, and 1073 (New Jersey margin) in the
125 Atlantic (Glass, 2002), DSDP Sites 65, 69, 70, 161, 162, 166, 167, and 292 in the equatorial
126 Pacific (Glass, 1985), and DSDP Site 216 in the NE Indian Ocean (Glass, 1985). They have also
127 been found in the South Atlantic at Maud Rise (ODP Site 689; Vonhof et al., 2000). These
128 microtektites include a large number of clinopyroxene-bearing spherules (Glass and Burns, 1988
129 termed these cpx-bearing spherules “microkrystites”) which characterize spherules from the
130 Pacific and South Atlantic. An iridium anomaly was reported to occur in association with these
131 ejecta (Asaro et al., 1982; Alvarez et al., 1982) but higher resolution work revealed that this Ir
132 anomaly occurs below the microtektite layer (Sanfilippo et al., 1985). This indicates that there
133 were actually two impacts at this time (Chesapeake and Popigai), one which produced an Ir
134 anomaly and microkrystites and a second which did not produce an Ir anomaly and which created
135 chemically distinct microtektites (Glass, 1985; Vonhof and Smit, 1999). The Ir anomaly is also
136 found at the Eocene-Oligocene Stratotype Section at Massignano, Italy, where it occurs ~ 12 m
137 below or ~1 myr before the base of the Oligocene (Montanari et al., 1993). Nevertheless, some
138 workers have inferred a causal relationship between these impacts and latest Eocene cooling and
139 faunal change (e.g., Keller, 1986; Vonhof et al., 2000; Liu et al., 2009), which would imply a
140 climate feedback which amplified the short-term cooling directly caused by the impact (Vonhof
141 et al., 2000).

142 **3 The Chicxulub Impact and Its Physical Effects**

143 The most important impact of the Phanerozoic, and the one which has been best studied by
144 scientific ocean drilling, is the Chicxulub impact. The hypothesis that an impact caused the most
145 recent major mass extinction was founded on elevated iridium levels in the K-Pg boundary clays
146 within outcrops in Spain, Italy, and Denmark (Smit and Hertogen, 1980; Alvarez et al., 1980). The
147 impact hypothesis was initially quite controversial, and one of the early objections was that iridium
148 had only been measured at a few sites across a relatively small area of western Europe and it may
149 have reflected a condensed interval and not a discrete impact (Officer and Drake, 1985).

150 Researchers then began to investigate and document other K-Pg boundary sites around the globe,
151 many of which were DSDP/ODP drill sites (Fig. 2). High iridium abundances were soon found at
152 other sites (e.g. Orth et al., 1981; Alvarez et al., 1982), and the identification of shocked minerals
153 within the K-Pg layer added irrefutable proof that it was formed by an extra-terrestrial impact
154 (Bohor et al., 1984). When a high-pressure shock wave passes through rocks, common minerals
155 such as quartz and feldspar are permanently deformed (referred to as shock metamorphism),
156 producing diagnostic features (e.g., Reimold et al., 2014) that, on Earth, are only found in
157 association with impacts and nuclear test sites. Since 1985, many ODP and IODP drill sites have
158 recovered (and often specifically targeted) the K-Pg boundary (Fig. 2), further contributing to our
159 understanding of this event, demonstrating that ejecta materials were deposited globally and
160 mapping their distribution (Figure 3).

161 The Chicxulub impact structure, on the Yucatán Peninsula, Mexico, was first identified as
162 a potential impact crater by Penfield and Carmargo (1981), and then as the site of the K-Pg impact
163 by Hildebrand et al. (1991). These authors noted that the size of the shocked quartz and thickness
164 of the K-Pg boundary deposit increased globally towards the Gulf of Mexico, and located the
165 Chicxulub crater due to its association with strong, circular, potential field gravity anomalies. Core
166 samples from onshore boreholes drilled by Petróleos Mexicanos (“Pemex”) confirmed its impact
167 origin. Although some authors have argued against a link between Chicxulub and the K-Pg
168 boundary (see Keller et al., 2004 and 2007 for mature forms of that position) accurate $^{40}\text{Ar}/^{39}\text{Ar}$
169 dating of impact glass within the K-Pg layer (Renne et al., 2013; 2018), as well as dating of and
170 microcrystalline melt rock (Swisher et al., 1992) and shocked zircon (Krogh et al., 1993; Kamo et
171 al., 2011) from Chicxulub and the K-Pg layer clearly demonstrate that Chicxulub is the site of the
172 K-Pg impact. Hildebrand et al. (1991) also noted that Gulf of Mexico DSDP Sites 94, 95, 536 and
173 540 contained deep water gravity flows and turbidity-current deposits adjacent to the Campeche
174 bank, and DSDP Sites 603B, 151 and 153, as well as outcrops along the Brazos River in Texas
175 had potential tsunami wave deposits (Bourgeois et al., 1988), all of which they suggested were
176 caused by the Chicxulub impact. Increasingly, opponents of the impact hypothesis have accepted
177 an end-Cretaceous age for the Chicxulub crater, and have focused their arguments on the Deccan
178 Traps in India as the sole or contributing cause of the mass extinction (see Chenet et al., 2009;
179 Mateo et al., 2014; and Keller et al., 2018 and references therein for a recent summary; Schulte et
180 al., 2010 remains the best rebuttal of these arguments).

181 Many studies have subsequently confirmed that, at sites proximal to Chicxulub, the impact
182 produced multiple resurge, tsunami, gravity flow and shelf collapse deposits (e.g. Bohor and
183 Betterton, 1993; Bralower et al., 1998; Grajales-Nishimura et al., 2000; Schulte et al., 2010; Hart
184 et al., 2012; Vellekoop et al., 2014). Well logs, DSDP cores, and seismic data show margin
185 collapse deposits reach 100s of meters thick locally, making the K-Pg deposit in the circum-Gulf
186 of Mexico the largest known single event deposit (Denne et al., 2013; Sanford et al., 2016).
187 Complex stratigraphy (Figure 3) and a mixture of nannofossil and foraminiferal assemblages of
188 different ages with impact-derived materials characterize proximal deep water DSDP and ODP
189 sites in the Gulf of Mexico (DSDP Sites 95, 535-538, and 540), and Caribbean (ODP Sites 999
190 and 1001) driven by the sequential deposition of material from seismically driven tsunami, slope
191 collapse, gravity flows and airfall (Bralower et al., 1998; Sigurdsson et al., 1997; Denne et al.,
192 2013; Sanford et al., 2016). This distinct assemblage of materials was termed the K-Pg “Boundary
193 Cocktail” by Bralower et al. (1998).

194 At intermediate distances from Chicxulub (2000-6000 km) the K-Pg boundary layer is 1.5
195 – 3 cm thick, as seen in North America (Smit et al., 1992; Schulte et al., 2010), Demerara Rise
196 (western Atlantic) ODP Site 1207 (MacLeod et al., 2007; Schulte et al., 2009), and Gorgonilla
197 Island, Columbia (Bermúdez et al., 2016). At the first two locations, it has a dual layer stratigraphy.
198 The lower layer contains goyazite and kaolinite spherules, which have splash-form morphologies
199 such as tear drops and dumbbells, and is overlain by the “boundary clay” containing the Ir anomaly
200 and Ni-rich spinels (Bohor et al., 1989; Smit and Romein, 1985; Bohor et al., 1993; Bohor and
201 Glass, 1995). The similarity between spherules in Haiti (~800 km from Chicxulub) and the lower
202 layer in North America has led to their joint interpretation as altered microtektites, which were
203 formed from ejected melt droplets (Smit and Romein, 1985; Sigurdsson et al., 1991; Bohor et al.,
204 1993; Bohor and Glass, 1995). Large-scale mass wasting has also been documented along the
205 North Atlantic margins of North America and Europe, including at Blake Plateau (ODP Site 1049),
206 Bermuda Rise (DSDP Sites 386 and 387), the New Jersey margin (DSDP Site 605), and the Iberian
207 Abyssal Plain (DSDP Site 398) (Klaus et al., 2000; Norris et al. 2000).

208 At distal sites (> 6000 km) the K-Pg boundary becomes a single layer with a fairly uniform
209 2-3 mm thickness, and has a similar chemical signature to the upper layer in North America (e.g.,
210 Alvarez et al. 1982; Rocchia et al., 1992; Montanari and Koeberl, 2000; Claeys et al., 2002). See,
211 for example, DSDP Site 738 on the southern Kerguelen Plateau (Thierstein et al., 1991), DSDP

212 Site 577 on Shatsky Rise (Zachos et al., 1985), DSDP Site 525 South Atlantic (Li and Keller,
213 1998); ODP Site 761 on Exmouth Plateau (Pospichal and Bralower, 1992); ODP Site 1262 on
214 Walvis Ridge (Bernaola and Monechi, 2007). The most abundant component (60-85%) of the
215 distal ejecta layer is spherules with a relict crystalline texture (Smit et al., 1992), which are referred
216 to as microkrystites (Glass and Burns, 1988), and are thought to have been formed from liquid
217 condensates within the expanding plume (Kyte and Smit, 1986). Ubiquitous alteration of these
218 microkrystites means that they are now primarily composed of clay (smectite, illite, and limonite).
219 Some spherules contain skeletal, magnesioferrite spinel (Smit and Kyte 1984; Kyte and Smit,
220 1986; Robin et al., 1991); spinel is the only pristine phase that appears to have survived diagenetic
221 alteration (Montanari et al., 1983; Kyte and Bostwick, 1995). Shocked minerals are present in the
222 K-Pg layer at all distances from Chicxulub, and are co-located with the elevated iridium (Smit,
223 1999).

224 DSDP, ODP, and IODP sites (Fig. 2) have all been used for mapping the global properties
225 of the K-Pg layer. Sites close to the crater appear to have a slightly lower total iridium flux at 10-
226 $45 \times 10^{-9} \text{ gcm}^{-2}$ (e.g. Rocchia et al., 1996; Claeys et al., 2002; MacLeod et al., 2007), as compared
227 to a global average of $\sim 55 \times 10^{-9} \text{ gcm}^{-2}$ (Kyte, 2004). Maximum iridium concentrations are quite
228 variable (< 1 to > 80 ppb, Claeys et al., 2002). Attempts have been made to locate the ultimate
229 source of the iridium, but the host is too fine-grained to be identified with conventional techniques.
230 Siderophile trace elements in the distal and upper K-Pg layer have a chondritic distribution (Kyte
231 et al., 1985), the isotopic ratio of the Platinum Group Element (PGE) osmium is extra-terrestrial
232 (Luck and Turekian, 1983; Meisel et al., 1995), and the chromium isotopic composition indicates
233 the impactor was a carbonaceous chondrite (Shukolyukov and Lugmair, 1998; Kyte, 1998).

234 The most common explanation for the origin of the microtektites at proximal and
235 intermediate sites is that they are formed from melted target rocks that have been ejected from
236 Chicxulub as melt droplets on a ballistic path within an ejecta curtain, and solidified en route to
237 their final destination (e.g., Pollastro and Bohor, 1993; Alvarez et al., 1995). Ejecta at distal sites
238 and within the upper layer at intermediate sites, including the shocked minerals and microkrystites,
239 are widely thought to have been launched on a ballistic trajectory from a rapidly expanding impact
240 plume (Argyle, 1989; Melosh et al., 1990). There are, however, several observations that are
241 difficult to reconcile with these explanations of the travel of K-Pg ejecta around the globe to its
242 final destination. For example: 1) microkrystites within the global layer have roughly the same

243 mean size (250 μm) and concentration (20,000 per cm^2) (Smit, 1999), whereas shocked minerals
244 show a clear decrease in number and size of grains with increasing distance from Chicxulub
245 (Hildebrand et al., 1991; Crookell et al., 2002); 2) if shocked quartz were ejected at a high enough
246 velocity to travel to the other side of the globe, the quartz would anneal on re-entry (Alvarez et al.,
247 1995; Crookell et al., 2002); and 3) if the lower layer at intermediate sites were formed from melt
248 droplets ejected from Chicxulub on a ballistic path, the thickness of the lower layer would decrease
249 with distance from Chicxulub whereas, across North America, but it is close to constant. The
250 interaction of re-entering ejecta with the Earth's atmosphere appears to be necessary to explain all
251 of these observations, with ejecta being re-distributed laterally by atmospheric heating and
252 expansion (Goldin and Melosh, 2007; 2008; Artemieva and Morgan 2009; Morgan et al., 2013).

253 Differences in the K-Pg boundary layer around the globe have been used to infer different
254 angles and directions for the Chicxulub impactor. Schultz and D'Hondt (1996) argued that several
255 factors, including the dual layer stratigraphy and particularly large fragments of shocked quartz in
256 North America, indicated an impact direction towards the northwest. However, comparable 2-cm
257 thick K-Pg layers at sites to the south of Chicxulub at equivalent paleodistances have been
258 identified (Schulte et al., 2009; Bermúdez et al., 2016), and it now appears that the ejecta layer is
259 roughly symmetric, with the number and size of shocked quartz grains decreasing with distance
260 from Chicxulub (Crookell et al., 2002; Morgan et al., 2006). One asymmetric aspect of the layer is
261 the spinel chemistry: spinel from the Pacific (e.g., DSDP Site 577) is characterized by higher Mg
262 and Al content than European (e.g., Gubbio, Italy) and Atlantic spinel (e.g., DSDP Site 524) (Kyte
263 and Smit, 1986). The Pacific spinel represented a higher temperature phase, and thus that the
264 impact direction must have been towards the west because the plume would be hottest in the
265 downrange direction (Kyte and Bostwick 1995). However, thermodynamic models of sequential
266 condensation within the cooling impact plume suggest the opposite: that the spinel from Europe
267 and the Atlantic represented the higher temperature phases and, thus, that the impact direction was
268 towards the east (Ebel and Grossman 2005). An argument that sought to use position of crater
269 topography relative to the crater center (Schultz and D'Hondt, 1996) has been questioned through
270 comparisons with Lunar and Venutian craters with known impact trajectories (Ekholm and
271 Melosh, 1998; McDonald et al., 2008). The best estimate to impact direction to date, based on 3D
272 numerical simulations of crater formation which incorporate new data from IODP Site M0077 in

273 the Chicxulub crater, indicates that an impact towards the southwest at a $\sim 60^\circ$ angle produces the
274 best match between the modeled and observed 3D crater structure (Collins et al., 2017).

275 **4 Ocean Drilling Perspective on Mass Extinction**

276 Paleontologists have long recognized a major mass extinction at the end of the Cretaceous
277 with the disappearance of non-avian dinosaurs, marine reptiles, and ammonites, although the first
278 indication of the rapidity of this event came from microfossils. The earliest studies of the extinction
279 of the calcareous microfossils across the K-Pg boundary came from outcrops on land (e.g.,
280 Luterbacher and Premoli-Silva, 1964; Perch Nielsen et al., 1982; Percival and Fischer, 1977;
281 Romein, 1977; Jiang and Gartner, 1986; Smit, 1982; Harwood, 1988; Hollis, 1997; Hollis et al.,
282 2003). However, the full taxonomic scope of the extinction and how it related to global
283 biogeography and ecology is largely known from ocean drilling (e.g., Thierstein and Okada, 1979;
284 Thierstein, 1982; MacLeod et al., 1997; Pospichal and Wise, 1990; Bown et al., 2004). Deep-sea
285 sites also serve as the basis for our understanding of the subsequent recovery of life (Bown, 2005;
286 Coxall et al., 2006; Bernaola and Monechi, 2007; Jiang et al., 2010; Hull and Norris, 2011; Hull
287 et al., 2011; Koutsoukos, 2014; Birch et al., 2016; Lowery et al., 2018). The K-Pg boundary has
288 been recovered in dozens of cores from all major ocean basins, including some from the earliest
289 DSDP legs (Fig. 2) (Premoli Silva and Bolli, 1973; Perch-Nielsen, 1977; Thierstein and Okada,
290 1979; see summary of terrestrial and marine K-Pg sections in Schulte et al., 2010). Deep-sea cores
291 generally afford excellent microfossil preservation, continuous recovery, and tight stratigraphic
292 control including magnetostratigraphy and orbital chronology (Röhl et al., 2001; Westerhold et al.,
293 2008).

294 Studies of deep-sea sections have exposed the severity of the mass extinction among the
295 calcareous plankton with over 90% of heterotroph foraminifera and autotroph nannoplankton
296 species becoming extinct (Thierstein, 1982; D'Hondt and Keller, 1991; Coxall et al., 2006; Hull
297 et al., 2011). The extinction was highly selective, with siliceous groups experiencing relatively
298 low rates of extinction (Harwood, 1988; Hollis et al., 2003). Among the calcareous plankton
299 groups, survivors include high-latitude and near-shore species (Bown, 2005; D'Hondt and Keller,
300 1991) suggesting that these species were adapted to survive variable environments in the
301 immediate aftermath of the impact. Benthic foraminifera survived the impact with little extinction
302 (Culver, 2003).

303 A key component of the post-extinction recovery of life is the recovery of primary
304 productivity. Photosynthesis favors ^{12}C over ^{13}C , enriching organic material in the former. Sinking
305 organic matter in the ocean removes ^{12}C from the upper water column; thus, under normal
306 conditions, there is a carbon isotope gradient from the surface waters to the seafloor. After the
307 Chicxulub impact, this vertical gradient collapsed for ~ 4 myr (e.g. Coxall et al., 2006). This
308 phenomenon which was originally interpreted as indicating the complete or nearly complete
309 cessation of surface ocean productivity (Hsü and McKenzie, 1985; Zachos et al., 1989; the latter
310 from DSDP Site 577 on Shatsky Rise), a hypothesis which became known as the Strangelove
311 Ocean (after the 1964 Stanley Kubrick movie) (Hsü and McKenzie, 1985). D'Hondt et al. (1998)
312 suggested that surface ocean productivity continued, but the extinction of larger organisms meant
313 that there was no easy mechanism (e.g., fecal pellets) to export this organic matter to the deep sea
314 – a modification of the Strangelove Ocean hypothesis that they called the Living Ocean hypothesis
315 (D'Hondt, 2005; see also Adams et al., 2004). The observed changes in carbon isotopes can be
316 explained by just a slight increase (from 90 to 95%) in the fraction of organic matter remineralized
317 in the upper ocean (D'Hondt et al., 1998; Alegret and Thomas, 2012), although others have
318 suggested a more precipitous drop in export productivity (Coxall et al., 2006). The lack of a
319 corresponding benthic foraminiferal extinction suggests that the downward flux of organic carbon
320 may have decreased somewhat but remained sufficiently elevated to sustain the benthic
321 community (Hull and Norris, 2011; Alegret et al., 2012). Research on barium fluxes in deep sea
322 sites across the oceans has shown that, in fact, export productivity was highly variable in the early
323 Danian, with some sites recording an *increase* in export production during the period of supposed
324 famine in the deep sea (Hull and Norris, 2011).

325 However, the shift in the surface-to-deep carbon isotope gradient does have significant
326 implications for biogeochemical cycling. The extinction of pelagic calcifiers like planktic
327 foraminifera and calcareous nannoplankton caused profound changes in the cycling of carbon from
328 the surface to the deep sea. Pelagic calcifiers are a key component of the carbon cycle, exporting
329 carbon in the form of CaCO_3 from the surface ocean to the seafloor. The near eradication of these
330 groups would have made surface to deep cycling less efficient, explaining the decreased carbon
331 isotope gradient (Hilting et al., 2008; Alegret et al. 2012; Henehan et al., 2016). This also led to
332 the weakening of the marine “alkalinity pump” (D'Hondt, 2005; Henehan et al., 2016), and the
333 resulting carbonate oversaturation can be observed overall improved carbonate preservation in the

334 deep sea as well as a white layer that overlies the K-Pg boundary in numerous sites including the
335 eastern Gulf of Mexico (DSDP Site 536; Buffler et al., 1984), the Caribbean (ODP Sites 999 and
336 1001; Sigurdsson et al., 1997), Shatsky Rise in the western Pacific (Fig. 3) (ODP Sites 1209-1212;
337 Bralower et al., 2002), and in the Chicxulub Crater itself (IODP Site M0077; Morgan et al., 2017).

338 Records from cores across the oceans indicate that the post-extinction recovery of export
339 productivity (e.g., Hull and Norris, 2011) and calcareous plankton diversity (e.g., Jiang et al., 2010)
340 were geographically heterogeneous, with some localities recovering rapidly and others taking
341 hundreds of thousands (for productivity) to millions (for diversity) of years to recover. Among the
342 nanoplankton, northern hemisphere assemblages are characterized by a series of high-dominance,
343 low-diversity “boom-bust” species (Bown, 2005); southern hemisphere assemblages contain a
344 somewhat more diverse group of surviving species (Schueth et al., 2015). In general, diversity of
345 northern hemisphere assemblages took longer to recover (Jiang et al., 2010). Recovery of export
346 productivity likewise appears to have been slower in the North Atlantic and Gulf of Mexico (e.g.,
347 Alegret et al., 2012; Jiang et al., 2010; Hull and Norris, 2011), suggesting that distance from the
348 crater correlates to slower recovery. Some authors (e.g., Jiang et al., 2010) attributed this to direct
349 environmental effects of the impact, such as perhaps the uneven distribution of toxic metals in the
350 oceans. If recovery is slower closer to the crater, then it should be slowest in the crater itself.
351 However, recent drilling within the Chicxulub crater itself has shown a rapid recovery of life, with
352 planktic and benthic organisms appearing within just a few years of the impact and a healthy, high
353 productivity ecosystem established within 30 kyr of the impact, much faster than estimates for
354 other Gulf of Mexico and N. Atlantic sites (Lowery et al., 2018). This rules out an environmental
355 driver for heterogeneous recovery and instead suggests that natural ecological factors including
356 incumbency and competitive exclusion (e.g., Hull et al., 2011; Schueth et al., 2015) and
357 morphospace reconstruction (Lowery and Fraass, 2018) were the dominant controls on the
358 recovery of the marine ecosystem. The recovery of diversity took millions of years to even begin
359 to approach Cretaceous levels (Coxall et al., 2006; Bown et al., 2004; Fraass et al., 2015). This
360 delay in the recovery of diversity appears to be a feature of all extinction events (Kirchner and
361 Weil, 2000; Alroy, 2008) and bodes ill for the recovery of the modern biosphere after negative
362 anthropogenic impacts associated with climate change, ocean acidification, hypoxia, etc. subside.

363 **5 Unique Insight into the Chicxulub Crater**

364 Joint IODP-ICDP Expedition 364 drilled into the peak ring of the Chicxulub impact crater
365 in 2016 at Site M0077 (Morgan et al., 2017). Peak rings have elevated topography that protrude
366 through the crater floor in the inner part of large impact structures. Prior to drilling, there was no
367 consensus on the nature of the rocks that form peak rings or their formational mechanism (Baker
368 et al., 2016). To form large craters like Chicxulub, rocks must temporarily behave in a fluid-like
369 manner during crater formation (Melosh, 1977; Riller et al., 2018). Two hypotheses, developed
370 from the observation of craters on other planets, provided possible explanations of the processes
371 by which peak rings form. The first, the dynamic collapse model (first put forward by Murray,
372 1980) predicted that the Chicxulub peak ring would be formed from deep crustal rock, presumably
373 crystalline basement. The second, the nested melt-cavity hypothesis (conceived by Cintala and
374 Grieve, 1998), predicted that the Chicxulub peak ring would be underlain by shallow crustal rock,
375 presumably Cretaceous carbonates. Thus, Expedition 364 was able to answer a major question
376 about impact cratering processes simply by seeing what rock comprises the peak ring (Figure 3).
377 Geophysical data acquired prior to drilling indicate that there are sedimentary rocks several
378 kilometers beneath the peak ring at Chicxulub, and that the peak-ring rocks have a relatively low
379 velocity and density, suggesting that they are highly fractured (Morgan et al., 1997; Morgan and
380 Warner, 1999; Gulick et al., 2008, 2013; Morgan et al., 2011).

381 The discovery that the peak ring was formed from fractured, shocked, uplifted basement
382 rocks supports the dynamic collapse model of peak-ring formation (Morgan et al., 2016; Kring et
383 al., 2017). Structural data from the wireline logging, CT scans, and visual core descriptions provide
384 an exceptional record of brittle and viscous deformation mechanisms within the peak-ring rocks.
385 These data reveal how deformation evolved during cratering, with dramatic weakening followed
386 by a gradual increase in rock strength (Riller et al., 2018). The peak-ring rocks have extraordinary
387 physical properties: the granitic basement has P-wave velocities and densities that are,
388 respectively, ~25% and ~10% lower than expected, and a porosity of 8-10%. These values are
389 consistent with numerical simulations that predict the peak-ring basement rocks represent some of
390 the most shocked and damaged rocks in an impact basin (Christeson et al., 2018). Site M0077
391 cores and measurements have been used to refine numerical models of the impact and new
392 estimates on the release of cooling climatic gases by the Chicxulub impact. Previous studies have
393 estimated that the Chicxulub impact released anywhere from 30-1,920 100 Gt of sulfur from the
394 evaporite-rich target rocks (this sulfur formed sulfate aerosols in the atmosphere, blocking

395 incoming solar radiation) (see Tyrrell et al., 2015 and references therein); a recent global climate
396 model indicates that a modest injection of 100 Gt S may have resulted in a 26°C drop in global
397 temperatures (Brugger et al., 2017). New impact models calibrated with data from Site M0077
398 suggest that between 195 and 455 Gt of sulfur were released, suggesting even more radical cooling
399 during the impact winter (Artemieva et al., 2017). However, it appears that only the most extreme
400 estimates of S release would have driven ocean acidification severe enough to explain the
401 extinction of calcareous plankton (Tyrrell et al., 2015), suggesting that the sharp reduction in
402 sunlight for photosynthesis drove the extinction.

403 **6 New Challenges**

404 The scientific community's understanding of the Chicxulub impact event and the K-Pg
405 mass extinction has grown immensely since Smit and Hertogen (1980) and Alvarez et al. (1980)
406 proposed the impact hypothesis, and many of the advances were the direct result of scientific ocean
407 drilling data. However, there is still a great deal that we do not know. New K-Pg boundary sites
408 from undersampled regions (the Pacific, the Indian Ocean, and the high latitudes) are essential to
409 reconstruct environmental gradients in the early Paleocene, understand geographic patterns of
410 recovery and what drives them. IODP Site U1514, on the Naturaliste Plateau on the SW Australian
411 margin (Fig. 2), was drilled in 2017 on Expedition 369 (Huber et al., 2018) and is a perfect example
412 of the kind of new site we need to drill; at a high latitude and far from existing K-Pg boundary
413 records.

414 New data from the Chicxulub Crater have resulted in refined impact models that suggest
415 that the asteroid impacted towards the southwest (Collins et al., 2017) which contrasts with
416 previously inferred directions that placed the northern hemisphere in the downrange direction.
417 Although the most proximal Pacific crust at the time of impact has since been subducted, very
418 little drilling has been conducted on older crust in the central and eastern Pacific (red circle on Fig.
419 2). New drilling on seamounts and rises on the easternmost Cretaceous crust in the equatorial
420 Pacific could shed new light on the environmental and biological consequences of being
421 downrange of the Chicxulub Impact, and may finally yield some fragments of the impactor.

422 Finally, the Chicxulub structure remains an important drilling target to address questions
423 that can only be answered at the K-Pg impact site. Additional drilling in the annular trough and
424 the central basin will likely bring the greatest return. IODP Site M0077, which was drilled at the

425 location where the peak ring was shallowest, recovered a relatively thin Paleocene section with an
426 unconformity present prior to the Paleocene-Eocene boundary. Seismic mapping within the crater
427 demonstrates that the Paleocene section greatly expands into the annular trough (Fig. 4), providing
428 an exciting opportunity to study the return of life to the impact crater at an even higher resolution
429 than Lowery et al. (2018). Additionally, continuous coring within an expanded Paleocene section
430 and the underlying impactites would better constrain climatologic inputs from the vaporization of
431 evaporites.

432 Equally intriguing is the interaction of impact melt rock, suevite, and post-impact
433 hydrothermal systems for studying how subsurface life can inhabit and evolve within an impact
434 basin. Such settings were common on early Earth and provide an analog for the chemical evolution
435 of pre-biotic environments as well as biologic evolution in extreme environments. Full waveform
436 images (Fig. 4) give tantalizing suggestions of vertical flux in the form of morphologic
437 complexities within the low-velocity suevite later above the high-velocity central melt sheet, which
438 are tempting to interpret as ancient hydrothermal vent systems of the kind often seen at mid-ocean
439 ridges. Drilling into the Chicxulub melt sheet would be ideal to study the hydrogeology and
440 geomicrobiology of impact melt sheets buried by breccias as a habitat for subsurface life, providing
441 an opportunity for scientific ocean drilling to sample the best analog for the habitat in which life
442 may have formed on early Earth and on rocky bodies across the solar system and beyond.

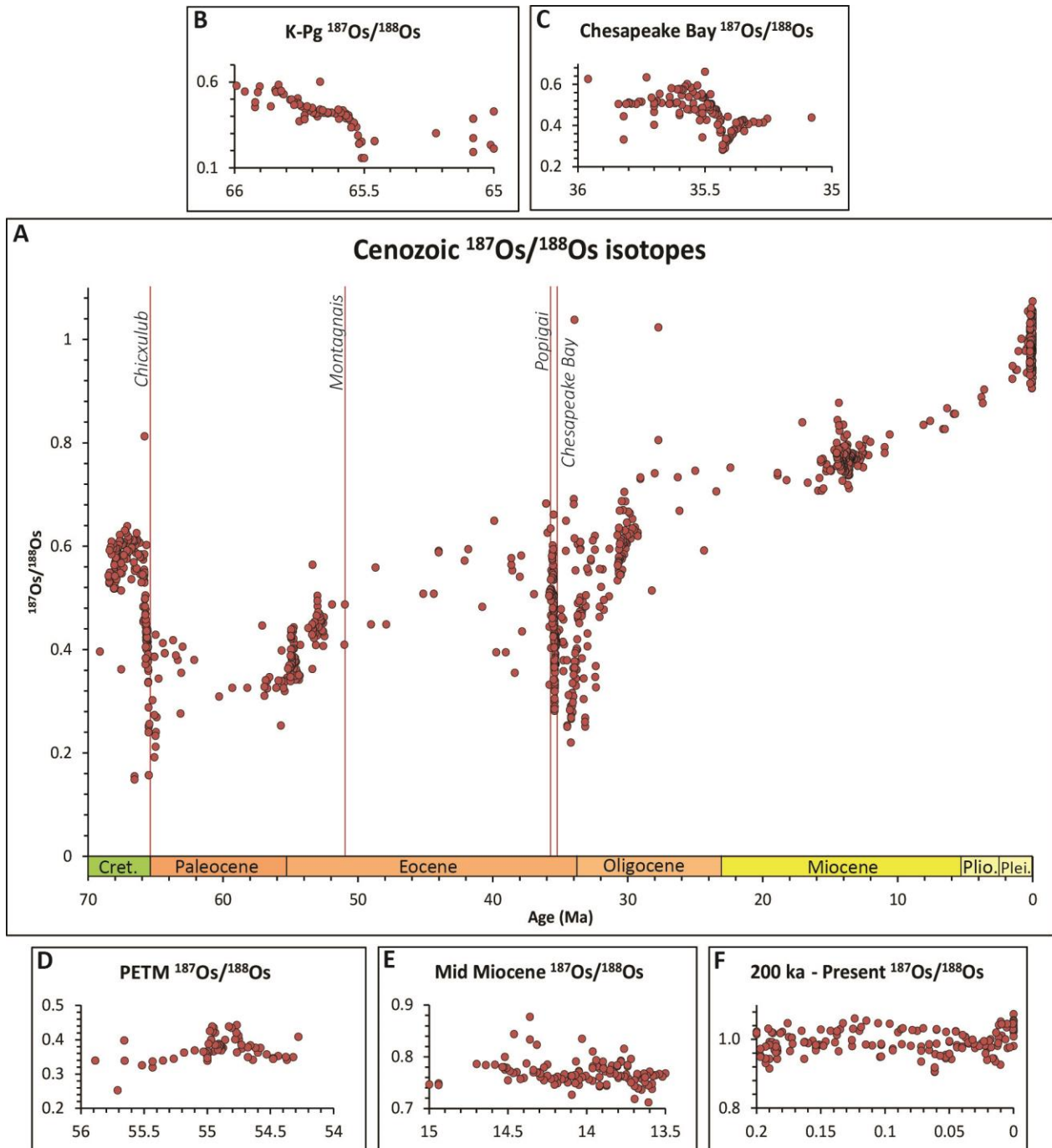
443 The success of the cooperation between IODP and ICDP during Expedition 364 serves as
444 a model for future drilling in the Chicxulub crater as well as future Mission Specific Platform
445 (MSP) expeditions. The onshore Yaxcopil-1 borehole unexpectedly encountered a Cretaceous
446 megablock because it was drilling with only the regional magnetic and gravity anomaly maps to
447 guide it. High-quality marine seismic data from offshore portion of the Chicxulub crater (Morgan
448 et al., 1997; Gulick et al., 2008; Christeson et al., 2018) allowed for a detailed characterization of
449 the subsurface before drilling even began (Whalen et al., 2013). In turn, this allowed Hole M0077A
450 to precisely target not just the peak ring but a small depression on top of the peak ring expected to
451 contain earliest Paleocene age sediments which provided the basis for unprecedented study of this
452 unique interval at ground zero (Lowery et al., 2018 and a number of upcoming papers). As we plan
453 for the next 50 years of scientific ocean drilling, we should look for additional opportunities to
454 leverage the clarity and resolution of marine seismic data with the precision drilling possible from

455 a stable platform provided by ICDP (Exp. 364 achieved essentially 100% recovery; Morgan et al.,
456 2017).

457

458

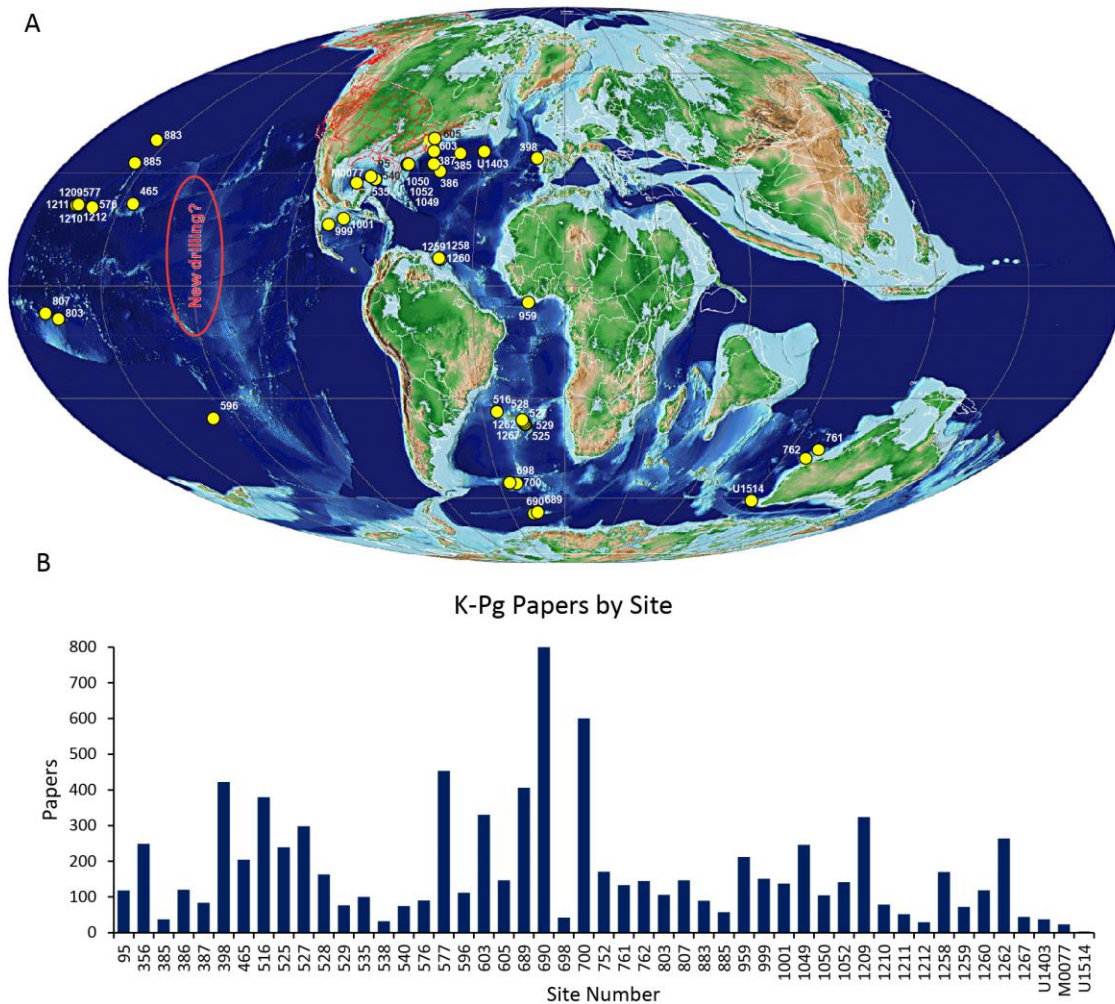
459



460

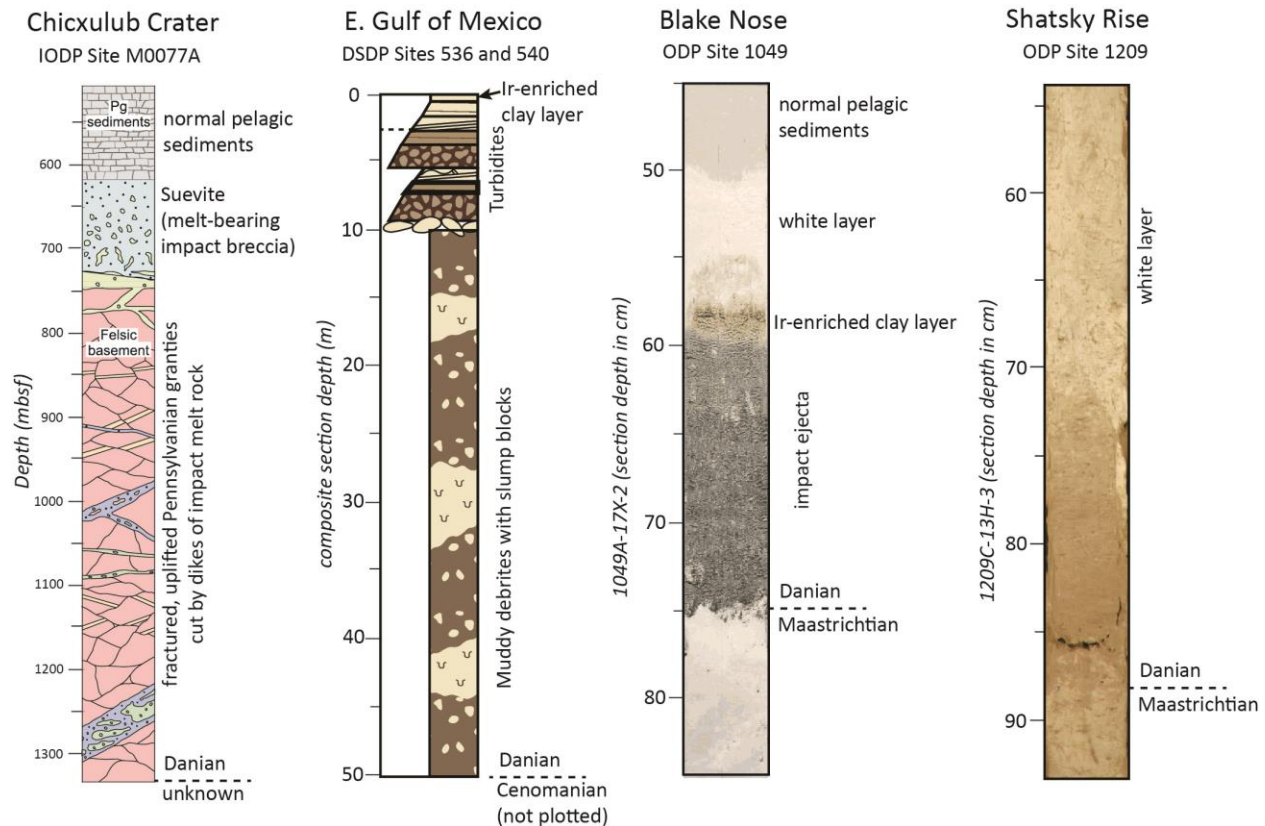
461 **Fig. 1** Marine osmium isotopes through the Cenozoic (a), after Peucker-Ehrenbrink and Ravizza
 462 (2012). These data, the majority of which come from DSDP/ODP/IODP cores, record the long-
 463 term trend toward more radiogenic (i.e., continental-weathering derived) $^{187}\text{Os}/^{188}\text{Os}$ ratios in the
 464 ocean throughout the Cenozoic. Superimposed on this long-term trend are several major, rapid
 465 shifts toward unradiogenic ratios driven by impact of extraterrestrial objects. This effect is evident
 466 in intervals associated with impact events, including the Chicxulub impact (b) and Chesapeake

467 Bay impact (c). Other intervals of major environmental change lack the diagnostic negative
 468 excursion, including the Paleocene Eocene Thermal Maximum (d), Miocene Climate Transition
 469 (e), and Younger Dryas (f). Red lines are well-dated large (>35 km crater diameter) impacts, after
 470 Grieve (2001). Note that these data are plotted against the 2012 Geologic Timescale (Peucker-
 471 Ehrenbrink and Ravizza, 2012); more recent dating puts the K-Pg boundary at 66.0 Ma (Renne et
 472 al., 2013).



473
 474 **Fig. 2 a)** Map of DSDP/ODP/IODP Sites which recovered the K-Pg boundary, up to Exp. 369.
 475 Basemap is adapted from the PALEOMAP Project (Scotese, 2008) **b)** Number of K-Pg papers by
 476 site, according to Google Scholar as of November 30, 2018. As anyone who’s searched for a paper
 477 on Google Scholar will recognize, there are some caveats with these data (e.g., inclusion of papers

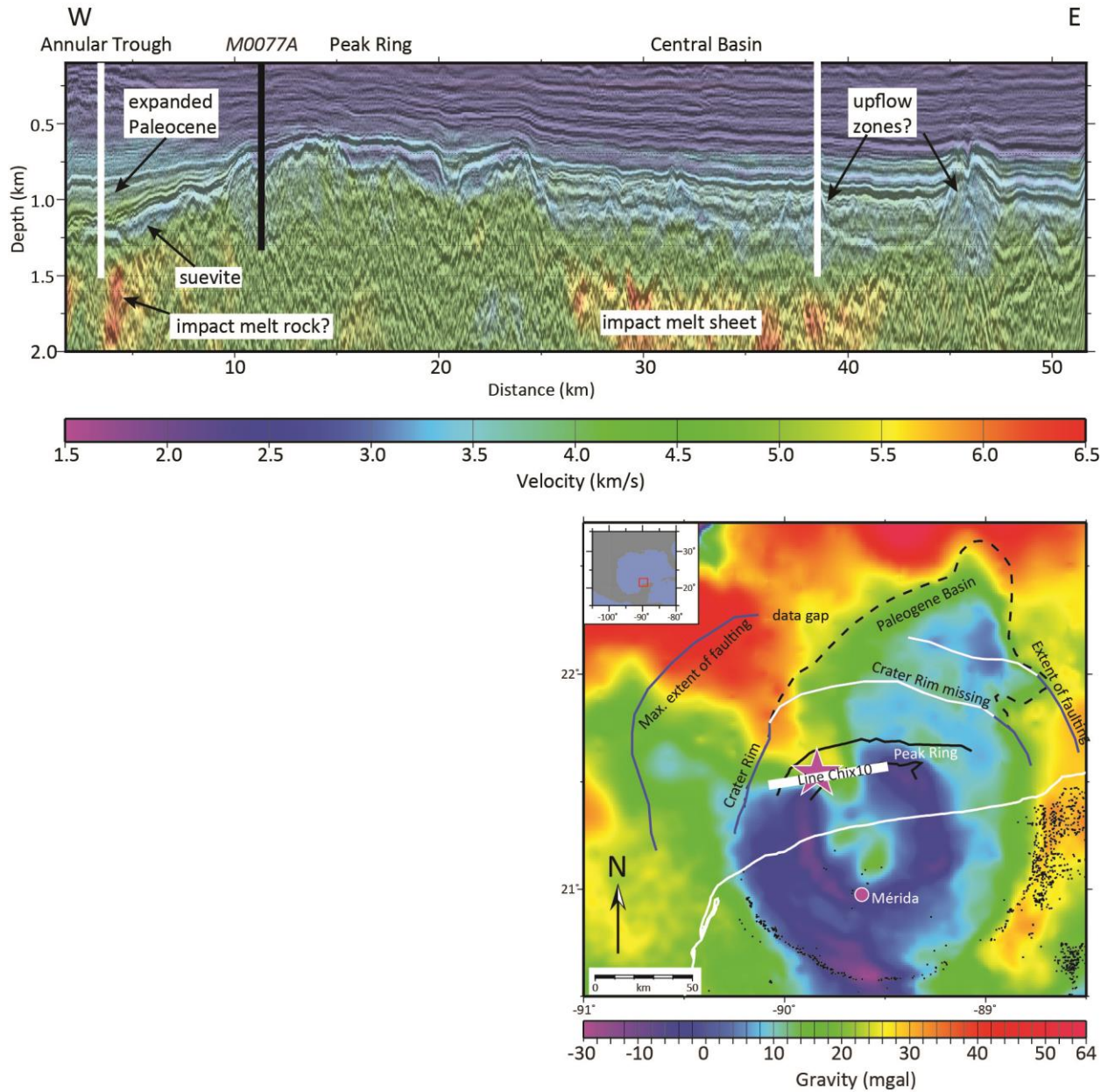
478 which match the search terms but are not strictly about the K-Pg, papers that are missing because
 479 they are not cataloged by Google Scholar, etc.). However, this is a good approximation of the
 480 reams of articles that have been written about the K-Pg from DSDP, ODP, and IODP cores, and
 481 the clear impact (sorry) of scientific ocean drilling on the K-Pg literature. n = 8679, but includes
 482 duplicates from papers which cover multiple sites. Search term: “Cretaceous AND Tertiary OR
 483 Paleogene OR Paleocene AND ‘Site ###’”. Most recent site is U1514 (n=3).



484

485 **Fig. 3** Representative K-Pg boundary sections from scientific ocean drilling cores. The peak ring
 486 of the Chicxulub crater itself shows pelagic post-impact sediments overlaying downward-
 487 coarsening suevite on top of impact melt rock, which in turn overlays fractured pre-impact granite
 488 cut by impact dikes (Morgan et al., 2016). Eastern Gulf of Mexico cores show the proximal deep-
 489 sea expression of the boundary layer, with massive slumps caused by platform margin collapse
 490 overlain by turbidites associated with secondary mass wasting, overlain by fallout of Ir-rich clay
 491 (Sanford et al., 2016). Blake Nose represents the dual-layer stratigraphy of many mid-distance
 492 localities, with impact ejecta overlain by an Ir-rich clay layer (Schulte et al., 2010). Shatsky Rise
 493 is typical of distal deep-sea sites, with a color change the only core-scale evidence of the impact

494 (Schulte et al., 2010). Chicxulub crater is redrawn from Morgan et al. (2016), eastern Gulf of
 495 Mexico is redrawn from Sanford et al. (2016), Blake Nose and Shatsky Rise core photographs are
 496 from the Janus database.



497
 498 **Fig. 4 (a)** Full wavefield inverted (FWI) velocity model (colors) and migrated seismic reflection
 499 image for profile CHIX 10 crossing site M0077 (black line). The seismic image has been converted
 500 to depth using the inverted velocity model. Potential sites for future drilling are shown with white
 501 lines. Drilling in the annular trough site would encounter an expanded Paleocene section, underlain

502 by suevite (low velocities) and possible impact melt rock (high velocities). Coring in the central
503 basin site would target an interpreted hydrothermal upflow zone (disrupted low-velocities) above
504 the impact melt sheet (high velocities) as well as an expanded Paleocene section. **(b)** Location map
505 showing the gravity-indicated structure of the crater and the position of the seismic line used in A.
506 Modified from Gulick et al. (2008).

507

508 **Acknowledgements.** We would like to thank the editors for inviting us to contribute to this special
509 issue, and Ellen Thomas and Mark Leckie for their thoughtful reviews. We are also grateful to
510 Bernhard Peucker-Ehrenbrink for sharing his Os isotope dataset and Ian Norton and Jeremy Owens
511 for their help with the paleogeographic map projection. We acknowledge NSF OCE 1737351 for
512 CL, TB, SG, and GC, and NERC NE/P005217/1 for JM. Finally, we gratefully acknowledge the
513 shipboard and shore-based scientists who worked to generate these data over the past 50 years of
514 scientific ocean drilling.

515

516 **Expedition 364 Scientists**

517 Tim Bralower, Elise Chenot, Gail Christeson, Philippe Claeys, Charles Cockell, Marco J. L.
518 Coolen, Ludovic Ferrière, Catalina Gebhardt, Kazuhisa Goto, Sophie Green, Sean Gulick,
519 Heather Jones, David A. Kring, Johanna Lofi, Christopher Lowery, Claire Mellett, Joanna
520 Morgan, Rubén Ocampo-Torres, Ligia Perez-Cruz, Annemarie Pickersgill, Michael Poelchau,
521 Auriol Rae, Cornelia Rasmussen, Mario Rebolledo-Vieyra, Ulrich Riller, Honami Sato, Jan
522 Smit, Sonia Tikoo, Naotaka Tomioka, Jaime Urrutia-Fucugauchi, Michael Whalen, Axel
523 Wittmann, Long Xiao, and Kosei Yamaguchi.

524

525

526 **References**

527 Abramov, O., & Kring, D.A., (2007). Numerical modeling of impact-induced hydrothermal
528 activity at the Chicxulub crater. *Meteoritics & Planetary Science*, 42, 93–112.
529 <http://dx.doi.org/10.1111/j.1945-5100.2007.tb00220.x>

530 Adams, J.B., Mann, M.E., & D'Hondt, S. (2004). The Cretaceous-Tertiary extinction: Modeling
531 carbon flux and ecological response. *Paleoceanography*, 19, PA1002,
532 doi:10.1029/2002PA000849

533 Alegret, L., & Thomas, E. (2005). Cretaceous/Paleogene boundary bathyal paleo-environments in
534 the central North Pacific (DSDP Site 465), the Northwestern Atlantic (ODP Site 1049), the
535 Gulf of Mexico and the Tethys: The benthic foraminiferal record. *Palaeogeography,*
536 *Palaeoclimatology, Palaeoecology*, 224, 53-82.

- 537 Alegret, L., Thomas, E., & Lohmann, K.C. (2012). End-Cretaceous marine mass extinction not
538 caused by productivity collapse, *Proceedings of the National Academy of Sciences*, 109,
539 728-732.
- 540 Alroy, J. (2008). Dynamics of origination and extinction in the marine fossil record, *Proceedings*
541 *of the National Academy of Sciences*, 105, 11536-11542.
- 542 Alvarez, L.W., Alvarez, W., Asaro, F., Michel, H.V., (1980). Extraterrestrial cause of the
543 Cretaceous–Tertiary extinction. *Science* 208, 1095–1108.
- 544 Alvarez, W., L.W. Alvarez, F. Asaro and H.V. Michel. (1982). Current status of the impact theory
545 for the terminal Cretaceous extinction. In L.T. Silver, L.T. & Schultz, P.H., eds.,
546 Geological implications of impacts of large asteroids and comets on the Earth, *GSA Special*
547 *Paper* 190, 305-315. Boulder, Colorado, Geological Society of America.
- 548 Alvarez, W., Claeys, P., Kieffer, S., (1995). Emplacement of Cretaceous–Tertiary boundary
549 shocked quartz from Chicxulub crater. *Science*, 269, 930–935.
- 550 Argyle, E. (1989). The global fallout signature of the K-T bolide impact. *Icarus*, 77, 220-222.
- 551 Artemieva, N., & Morgan, J. (2009), Modeling the formation of the K-Pg boundary layer, *Icarus*,
552 201, 768-780.
- 553 Artemieva N. et al., (2017), Quantifying the release of climate-active gases by large meteorite
554 impacts with a case study of Chicxulub, *Geophysical Research Letters*, ISSN: 0094-8276
- 555 Baker, D.M.H., Head, J.W., Collins, G.S., & Potter, R.W.K. (2016). The formation of peak-ring
556 basins: Working hypotheses and path forward in using observations to constrain models of
557 impact-basin formation, *Icarus*, 273, 146.
- 558 Bermúdez, H.D., García, J., Stinnesbeck, W., Keller, G., Rodríguez, J.V., Hanel, M., Hopp, J.,
559 Schwarz, W.H., Trieloff, M., Bolivar, L., & Vega, F.J., (2016), The Cretaceous-Palaeogene
560 boundary at Gorgonilla Island, Colombia, South America: *Terra Nova*, 28, 83–90,
561 <https://doi.org/10.1111/ter.12196>
- 562 Bernaola, G., & Monechi, S. (2007), Calcareous nannofossil extinction and survivorship across
563 the Cretaceous– Paleogene boundary at Walvis Ridge (ODP Hole 1262C, South Atlantic
564 Ocean), *Palaeogeography, Palaeoclimatology, Palaeoecology*, 255, 132-156.
- 565 Birch, H.S., Coxall, H.K., Pearson, P.N., Kroon, D., & Schmidt, D.N. (2016). Partial collapse of
566 the marine carbon pump after the Cretaceous-Paleogene boundary. *Geology*, 44, 287-290.
- 567 Bohor, B.F., Foord, E.E., Modreski, P.J., & Triplehorn, D.M., (1984). Mineralogic evidence for
568 an impact event at the Cretaceous–Tertiary boundary. *Science* 224, 867–869.
- 569 Bohor, B.F., Foord, E.E., & Betterton, W.J. (1989) Trace minerals in K-T boundary clays:
570 *Meteoritics* 24, 253.
- 571 Bohor, B.F. & Betterton, W.J., (1993). Arroyo el Mimbral, Mexico, K/T unit; origin as debris
572 flow/ turbidite, not a tsunami deposit. *Proceedings of the Lunar and Planetary Science*
573 *Conference*, 24, 143-144.

- 574 Bohor, B.F., Betterton, W.J., & Krogh, T.E., (1993). Impact-shocked zircons: discovery of shock-
575 induced textures reflecting increasing degrees of shock metamorphism. *Earth and*
576 *Planetary Science Letters*, 119, 419–424.
- 577 Bohor B.F. & Glass B.P. (1995) Origin and diagenesis of K/T impact spherules – From Haiti to
578 Wyoming and beyond. *Meteoritics*, 30, 182–198.
- 579 Bottomley, R., Grieve, R., York, D., & Masaitis, V. (1997). The age of the Popigai impact event
580 and its relation to events at the Eocene/Oligocene boundary. *Nature*, 388, 365.
- 581 Bourgeois J., Hansen T.A., Wiberg P.L., & Kauffman E.G. (1988) A tsunami deposit at the
582 cretaceous-tertiary boundary in Texas. *Science* 241. 567–570.
- 583 Bown, P. (2005), Selective calcareous nannoplankton survivorship at the Cretaceous-Tertiary
584 boundary, *Geology*, 33, 653-656.
- 585 Bown, P.R., J.A. Lees, and J.R. Young (2004), Calcareous nannoplankton evolution and diversity
586 through time, *Coccolithophores*, 481-508, Springer.
- 587 Bralower, T., Paull, C.K., & Leckie, R.M., (1998). The Cretaceous–Tertiary boundary cocktail:
588 Chicxulub impact triggers margin collapse and extensive gravity flows. *Geology* 26, 331–
589 334.
- 590 Bralower, T.J., Silva, I.P. & Malone, M.J., (2002). New evidence for abrupt climate change in the
591 Cretaceous and Paleogene: An Ocean Drilling Program expedition to Shatsky Rise,
592 northwest Pacific. *GSA TODAY*, 12, pp.4-10.
- 593 Buffler, R.T., Schlager, W., Pisciotto, K.A., & Leg 77 Scientists (1984). *Initial Reports of the Deep*
594 *Sea Drilling Project 77* Washington.
- Christeson et. al., (2018). Extraordinary Rocks from the Peak Ring of the Chicxulub Impact Crater:
P-Wave Velocity, Density, and Porosity Measurements from IODP/ICDP Expedition 364,
Earth and Planetary Science Letters, 495, 1-11.
- Cintala, M.J., and Grieve, R.A. (1998). Scaling impact melting and crater dimensions: Implications
for the lunar cratering record. *Meteoritics & Planetary Science*, 33, 889-912.
- 595 Claeys, P., Kiessling, W., & Alvarez, W., 2002. Distribution of Chicxulub ejecta at the Cretaceous–
596 Tertiary boundary. In: Koeberl, C. & MacLeod, K.G. (Eds.), *Catastrophic Events and Mass*
597 *Extinctions; Impacts and Beyond: Geological Society of America Special Paper*, 356, 55–
598 68.
- 599 Collins, G.S., N. Patel, A.S. Rae, T.M. Davies, J.V. Morgan, S.P.S. Gulick & Expedition 364
600 Scientists (2017), Numerical Simulations of Chicxulub crater formation by oblique impact,
601 *Lunar Planet. Sci. Conf. XLVII*, abstr # 1832.
- 602 Coxall, H.K., S. D'Hondt, & J.C. Zachos (2006), Pelagic evolution and environmental recovery
603 after the Cretaceous-Paleogene mass extinction, *Geology*, 34, 297-300.
- 604 Croskell, M., Warner, M., & Morgan, J. (2002). Annealing of shocked quartz during atmospheric
605 reentry. *Geophysical Research Letters*, 29, 1940–1944.
- 606 Culver, S.J. (2003). Benthic foraminifera across the Cretaceous–Tertiary (K–T) boundary: a
607 review. *Marine Micropaleontology*, 47, 177-226.

- 608 D'Hondt, S., & Keller, G. (1991). Some patterns of planktic foraminiferal assemblage turnover at
609 the Cretaceous-Tertiary boundary. *Marine Micropaleontology*, 17, 77-118.
- 610 D'Hondt, S., Donaghay, P., Zachos, J.C., Luttenberg, D., & Lindinger, M. (1998). Organic carbon
611 fluxes and ecological recovery from the Cretaceous-Tertiary mass extinction. *Science*, 282,
612 276-279.
- 613 D'Hondt, S. (2005). Consequences of the Cretaceous/Paleogene mass extinction for marine
614 ecosystems. *Annual Reviews of Ecology, Evolution, and Systematics*, 36, 295-317.
- 615 Denne, R.A., Scott, E.D., Eickhoff, D.P., Kaiser, J.S., Hill, R.J., & Spaw, J.M. (2013). Massive
616 Cretaceous-Paleogene boundary deposit, deep-water Gulf of Mexico: New evidence for
617 widespread Chicxulub-induced slope failure. *Geology*, 41, 983-986.
- 618 Ebel D.S. & L. Grossman, (2005), Spinel-bearing spherules condensed from the Chicxulub impact-
619 vapor plum, *Geology* 33, 293-296, DOI: 10.1130/G21136.1
- 620 Ekholm, A.G., & H.J. Melosh (2001), Crater features diagnostic of oblique impacts: The size and
621 position of the central peak, *Geophysical Research Letters*, 28, 623– 626.
- 622 Fraass, A.J., Kelly, D.C., & Peters, S.E. (2015). Macroevolutionary history of the planktic
623 foraminifera. *Annual Review of Earth and Planetary Sciences*, 43, 139-166.
- 624 Glass B.P., & Burns C.A., (1988), Mikrokrystites: a new term for impact-produced glassy
625 spherules containing primary crystallites, In: *Proceedings of Lunar and Planetary Science
626 Conference*, 18, 455-458.
- 627 Gohn, G.S., Koeberl, C., Miller, K.G., Reimold, W.U., Browning, J.V., Cockell, C.S., et al. (2008).
628 Deep drilling into the Chesapeake Bay impact structure. *Science*, 320, 1740-1745.
- 629 Goldin T.J. & Melosh H.J. (2007). Interactions between Chicxulub ejecta and the Atmosphere:
630 The Deposition of the K/T Double Layer. *38th Lunar and Planetary Science Conference*,
631 2114, #1338.
- 632 Goldin & Melosh, 2008. Chicxulub ejecta distribution, patchy or continuous? *39th Lunar and
633 Planetary Science Conference*, #2469.
- 634 Gulick, S.P.S., G.L. Christeson, P.J. Barton, R.A.F. Grieve, J.V. Morgan, & J. Urrutia-Fucugauchi
635 (2013), Geophysical characterization of the Chicxulub impact crater, *Reviews of
636 Geophysics*, 51, 31-52, doi: 10.1002/rog.200007.
- 637 Gulick, S.P.S. et al. (2016), *Expedition 364 Preliminary Report: Chicxulub: Drilling the K-Pg
638 Impact Crater*, International Ocean Discovery Program, doi:10.14379/iodp.pr364.2017
- 639 Grajales-Nishimura, Cedillo-Pardo, E., Rosales-Domínguez, C., Morán-Zenteno, D.J., Alvarez,
640 W., Claeys, P., Ruíz-Morales, J., García-Hernández, J., Padilla-Avila, P., & Sánchez-Ríos,
641 A., (2000), Chicxulub impact: The origin of reservoir and seal facies in the southeastern
642 Mexico oil fields, *Geology*, 28, 307–310.
- 643 Hart, M.B., Yancey, T.E., Leighton, A.D., Miller, B., Liu, C., Smart, C.W., & Twitchett, R.J.
644 (2012). The Cretaceous-Paleogene boundary on the Brazos River, Texas: New
645 stratigraphic sections and revised interpretations. *GCAGS Journal*, 1 69-80.

- 646 Harwood, D.M. (1988), Upper Cretaceous and lower Paleocene diatom and silicoflagellate
647 biostratigraphy of Seymour Island, eastern Antarctic Peninsula, *Geological Society of*
648 *America Memoirs*, 169, 55-130.
- 649 Henehan, M.J., P.M. Hull, D.E. Penman, J.W. Rae, & D.N. Schmidt (2016), Biogeochemical
650 significance of pelagic ecosystem function: an end-Cretaceous case study, *Phil. Trans. R.*
651 *Soc. B*, 371(1694), 20150510.
- 652 Hildebrand, A.R., Penfield, G.T., Kring, D.A., Pilkington, M., Camargo, A.Z., Jacobsen, S.B., &
653 Boynton, W.V., 1991. Chicxulub Crater: a possible Cretaceous/Tertiary boundary impact
654 crater on the Yucatán Peninsula, Mexico. *Geology*, 19, 867–871.
- 655 Hildebrand, A.R., et al. (1998), Mapping Chicxulub crater structure with overlapping gravity and
656 seismic surveys, *Proc. Lunar Planet Sci Conf.*, 29, 1821.
- 657 Hilting, A., Kump, L.R., & Bralower, T.J. (2007), Variations in the Oceanic Vertical Carbon
658 Isotope Gradient and Their Implications for the Paleocene-Eocene Biological Pump,
659 *Paleoceanography*, 23 PA3222, doi:10.1029/2007PA001458.
- 660 Hollis, C.J. (1997), Cretaceous-Paleocene Radiolaria from eastern Marlborough, New Zealand,
661 *Institute of Geological & Nuclear Sciences Monograph* 17, 1-152.
- 662 Hollis, C.J., & Strong, C.P. (2003). Biostratigraphic review of the Cretaceous/Tertiary boundary
663 transition, mid-Waipara river section, North Canterbury, New Zealand. *New Zealand*
664 *Journal of Geology and Geophysics*, 46 (2), 243-253.
- 665 Hsü, K.J., & McKenzie, J.A. (1985). A “Strangelove” ocean in the earliest Tertiary. *The Carbon*
666 *Cycle and Atmospheric CO: Natural Variations Archean to Present*, 487-492.
- 667 Huber, B.T., Hobbs, R.W., & Bogus, K.A. (2018). Tectonic, paleoclimate, and paleoceanographic
668 history of high-latitude southern margins of Australia during the Cretaceous. *Expedition*
669 *369 Preliminary Report: Australia Cretaceous climate and tectonics*. International Ocean
670 Discovery Program.
- 671 Hull, P.M., & R.D. Norris (2011), Diverse patterns of ocean export productivity change across the
672 Cretaceous-Paleogene boundary: New insights from biogenic barium, *Paleoceanography*,
673 26(3).
- 674 Hull, P.M., R.D. Norris, T.J. Bralower, & J.D. Schueth (2011), A role for chance in marine
675 recovery from the end-Cretaceous extinction, *Nature Geoscience*, 4, 856.
- 676 Jiang, M. J., & Gartner, S. (1986). Calcareous nannofossil succession across the
677 Cretaceous/Tertiary boundary in east-central Texas. *Micropaleontology*, 232-255.
- 678 Jiang, S., T.J. Bralower, M.E. Patzkowsky, L.R. Kump, & J.D. Schueth (2010), Geographic
679 controls on nannoplankton extinction across the Cretaceous/Palaeogene boundary, *Nature*
680 *Geoscience*, 3, 280.
- 681 Kamo, S.L., Lana. C., & Morgan, J.V., (2011) U–Pb ages of shocked zircon grains link distal K–
682 Pg boundary sites in Spain and Italy with the Chicxulub impact, *Earth and Planetary*
683 *Science Letters* 310 401–408.

- 684 Kasting, James F., (1993) Earth's early atmosphere. *Science* 259, 920-926.
- 685 Keller, G., Adatte, T., Stinnesbeck, W., Rebolledo-Vieyra, M., Urrutia-Fucugauchi, J., Kramar,
686 U., & Stüben, D., 2004. Chicxulub impact predates the K–T boundary mass extinction.
687 *Proceedings of the National Academy of Sciences*, 101, 3753–3758.
- 688 Keller, G., Adatte, T., Berner, Z., Harting, M., Baum, G., Prauss, M., Tantawy, A., & Stueben, D.,
689 2007, Chicxulub impact predates K–T boundary, new evidence from Brazos, Texas, *EPSL*
690 255, 339-356.
- 691 Kennett, D.J., Kennett, J.P., West, A., Mercer, C., Hee, S.Q., Bement, L., Bunch, T.E., Sellers, M.
692 & Wolbach, W.S., (2009). Nanodiamonds in the Younger Dryas boundary sediment layer.
693 *Science*, 323, 94-94.
- 694 Kirchner, J.W., & Weil, A. (2000). Delayed biological recovery from extinctions throughout the
695 fossil record *Nature* 404, 177-180.
- 696 Klaus, A., R.D. Norris, D. Kroon, & J. Smit (2000), Impact-induced mass wasting at the KT
697 boundary: Blake Nose, western North Atlantic, *Geology*, 28, 319-322.
- 698 Koeberl C. (1998). Identification of meteoritic component in impactites. In *Meteorites: Flux with*
699 *time and impact effects*, edited by Grady M. M., Hutchinson R., McCall G. J. H., and
700 Rothery R. A. London: The Geological Society. pp. 133–153.
- 701 Koeberl, C., Milkereit, B., Overpeck, J. T., Scholz, C. A., Amoako, P. Y. O., Boamah, D., et al.
702 (2007). An international and multidisciplinary drilling project into a young complex impact
703 structure: The 2004 ICDP Bosumtwi impact crater, Ghana, drilling project – An overview.
704 *Meteorit. Planet. Sci.*, 42, 483-511.
- 705 Kring, D.A., (2000) Impact events and their effect on the origin, evolution, and distribution of life,
706 *GSA Today* 10, 1–7.
- 707 Kring, D.A., Environmental consequences of impact cratering events as a function of ambient
708 conditions on Earth, (2003), *Astrobiology* 3, 133–152.
- 709 Kring, D.A., et al. (2017), Chicxulub and the exploration of large peak-ring impact craters through
710 scientific drilling, *GSA Today*, 27, 4-8.
- 711 Krogh, T.E., Kamo, S.L., & Bohor, B.F., (1993). U–Pb ages of single shocked zircons linking
712 distal K–T ejecta to the Chicxulub crater. *Nature* 366, 731–734.
- 713 Kump, L.R. (1991), Interpreting carbon-isotope excursions: Strangelove oceans, *Geology*, 19,
714 299-302.
- 715 Kyte, F.T., Smit, J., & Wasson, J.T., (1985). Siderophile inter-element variation in the Cretaceous–
716 Tertiary boundary sediments from Caravaca, Spain. *Earth and Planetary Science Letters*.
717 73, 183–195.
- 718 Kyte, F.T. & J. Smit. (1986). Regional variations in spinel compositions; an important key to the
719 Cretaceous/ Tertiary event. *Geology*, 14, 485-487.

- 720 Kyte F.T, & Bostwick J.A. (1995). Magnesioferrite spinel in Cretaceous/Tertiary boundary
721 sediments of the Pacific basin: remnants of hot, early ejecta from the Chicxulub impact?
722 *Earth and Planetary Science Letters* 132, 113–27.
- 723 Kyte, F.T. (1998), A meteorite from the Cretaceous/Tertiary boundary, *Nature*, 396(6708), 237.
- 724 Kyte, F.T., (2004). Primary mineralogical and chemical characteristics of the major K/T and Late
725 Eocene impact deposits. *AGU Fall Meeting abstract* #B33C-0272.
- 726 Lowery, C.M. et al., (2018), Rapid Recovery of Life At Ground Zero of the End Cretaceous Mass
727 Extinction, *Nature* v. 558, p. 288-291, <https://doi.org/10.1038/s41586-018-0163-6>
- 728 Lowery, C.M., & Fraass, A.J. (2018). Explanation for Delayed Recovery of Species Diversity
729 Following the End Cretaceous Mass Extinction. *PaleorXiv Preprint*.
730 <https://doi.org/10.31233/osf.io/wn8g6>
- 731 Luck, J.M., & Turekian, K.K. (1983). Osmium-187/Osmium-186 in manganese nodules and the
732 Cretaceous-Tertiary boundary. *Science*, 222, 613-615.
- 733 Luterbacher H.P & Premoli Silva I. (1964) - Biostratigrafia del limite Cretaceo-Terziario
734 nell'Apennino Centrale. *Riv. It. Paleont. Strat.*, 70, p. 67-128, Milano.
- 735 MacLeod, N., P. Rawson, P. Forey, F. Banner, M. Boudagher-Fadel, P. Bown, J. Burnett, P.
736 Chambers, S. Culver, & S. Evans (1997), The Cretaceous-tertiary biotic transition, *Journal*
737 *of the Geological Society*, 154, 265-292.
- 738 MacLeod, K.G., Whitney, D.L., Huber, B.T., & Koeberl, C., (2007). Impact and extinction in
739 remarkably complete Cretaceous-Tertiary boundary sections from Demerara Rise, tropical
740 western North Atlantic. *Geological Society of America Bulletin*, 119, pp.101-115.
- 741 McDonald, M.A., H.J. Melosh, & S.P.S. Gulick (2008), Oblique impacts and peak ring position:
742 Venus and Chicxulub, *Geophysical Research Letters*, 35, L07203,
743 doi:10.1029/2008GL033346, 2008
- 744 Meisel, T, Kraehenbuehl, U., & Nazarov, M.A.. 1995. Combined osmium and strontium isotopic
745 study of the Cretaceous-Tertiary boundary at Sumbar, Turkmenistan; a test for an impact
746 versus a volcanic hypothesis. *Geology*, 23, 4, 313-316.
- 747 Melles, M., Brigham-Grette, J., Minyuk, P. S., Nowaczyk, N. R., Wennrich, V., DeConto, R. M.,
748 et al. (2012). 2.8 Million Years of Arctic Climate Change from Lake El'gygytgyn, NE
749 Russia. *Science*, 337, 315.
- 750 Melosh, H.J. (1977) *Impact and Explosion Cratering* Pergamon Press.
- 751 Melosh, H.J., Schneider, N.M., Zahnle, K.J., & Latham, D. (1990), Ignition of global wildfires at
752 the Cretaceous-Tertiary boundary, *Nature*, 343, 251-254.
- 753 Meredith, Robert W., Janecka, J.E., Gatesy, J., Ryder, O.A., Fisher, C.A., Teeling, E.C., Goodbla,
754 A., et al. (2011) Impacts of the Cretaceous Terrestrial Revolution and KPg extinction on
755 mammal diversification. *Science* 1211028.
- 756 Michel, H.V., Asaro, F., Alvarez, W., & Alvarez L.W. (1986), 12. Geochemical studies of the
757 Cretaceous-Tertiary Boundary in ODP holes 689B and 906C1, *Proceedings of the Ocean*
758 *Drilling Program: Scientific Results* 113.

- 759 Montanari, A., Hay, R.L., Smit, J. et al., (1983). Spheroids at the Cretaceous-Tertiary boundary
760 are altered impact droplets of basaltic composition. *Geology*, 11, 668-671.
- 761 Montanari, A. & Koeberl, C., (2000). Impact Stratigraphy: The Italian Record. *Lecture and Notes*
762 *in Earth Sciences*. Springer-Verlag, Berlin. 364 pp.
- 763 Morgan, J., Warner, M., Brittan, J., Buffler, R., Camargo, A., Christeson, G. & Mackenzie, G.
764 (1997). Size and morphology of the Chicxulub impact crater. *Nature*, 390, 472-476.
- 765 Morgan, J., & Warner, M. (1999). Chicxulub: The third dimension of a multi-ring impact
766 basin. *Geology*, 27, 407-410.
- 767 Morgan J.V., Lana C., Kearsley A., Coles B., Belcher C., Montanari S., Di'az-Martí'nez E.,
768 Barbosa A. & Neumann V. (2006) Analyses of shocked quartz at the global K-P boundary
769 indicate an origin from a single, high-angle, oblique impact at Chicxulub. *Earth and*
770 *Planetary Science Letters*. 251, 264-279.
- 771 Morgan, J.V. (2008). Comment on "Determining Chondritic Impactor Size from the Marine
772 Osmium Isotope Record." *Science*, 321, 1158.
- 773 Morgan J., Artemieva N., & Goldin T., (2013), Revisiting wildfires at the K-Pg boundary, *Journal*
774 *of Geophysical Research: Biogeosciences*, 118, 1508-1520.
- 775 Morgan J.V. et al., (2016), The formation of peak rings in large impact craters, *Science*, 354, 878-
776 882.
- 777 Morgan, J.V., S.P.S. Gulick, C.L. Mellet, S.L. Green, and Expedition 364 Scientists (2017)
778 *Chicxulub: Drilling the K-Pg Impact Crater, Proceedings of the International Ocean*
779 *Discovery Program*, 364, International Ocean Discovery Program, College Station, TX,
780 doi: 10.14379/iodp.proc.364.103.2017.
- 781 Murray, J.B. (1980). Oscillating peak model of basin and crater formation. *The moon and the*
782 *planets*, 22, 269-291.
- 783 Nisbet, E.G., & Sleep, N.H., (2001). The habitat and nature of early life. *Nature* 409, 1083.
- 784 Norris, R. D., Firth, J., Blusztajn, J.S., & Ravizza, G. (2000), Mass failure of the North Atlantic
785 margin triggered by the Cretaceous-Paleogene bolide impact, *Geology*, 28, 1119-1122.
- 786 Officer, C.B. & Drake, C.L. (1985). Terminal Cretaceous environmental events. *Science*, 227,
787 1161-1167.
- 788 Orth, C. J., Gilmore, J.S., Knight, J.D., Pillmore, C.L., Tschudy, R.H., & Fassett, J.E. (1981), An
789 iridium abundance anomaly at the palynological Cretaceous-Tertiary boundary in northern
790 New Mexico. *Science*, 214, 1341-1343.
- 791 Paquay, F.S., Ravizza, G.E., Dalai, T.K., and Peucker-Ehrenbrink, B. (2008). Determining
792 chondritic impactor size from the marine osmium isotope record. *Science*, 320, 214-218.
- 793 Penfield, G.T., & Camargo-Zanoguera, A. (1981) Definition of a major igneous zone in the central
794 Yucatan platform with aeromagnetism and gravity, in *Technical Program, Abstracts and*
795 *Bibliographies, 51st Annual Meeting*, 37, Society of Exploration Geophysicists, Tulsa,
796 Oklahoma.

- 797 Perch-Nielsen, K. (1977), Albian to Pleistocene calcareous nannofossils from the western South
798 Atlantic, DSDP Leg 39, *Initial Reports of the Deep Sea Drilling Project*, 39, 699-823.
- 799 Perch-Nielsen, K., McKenzie, J., & He, Q. (1982), Biostratigraphy and isotope stratigraphy and
800 the ‘catastrophic’ extinction of calcareous nannoplankton at the Cretaceous/Tertiary
801 boundary, in Geological implications of impacts of large asteroids and comets on the Earth,
802 *GSA Special Paper* 190, 353-371.
- 803 Percival, S.F. & Fischer, A.G. (1972), Changes in calcareous nanno-plankton in the Cretaceous-
804 Tertiary biotic crisis at Zumay, Spain, *Evolutionary Theory* 2, 1-35.
- 805 Peucker-Ehrenbrink, B., & Ravizza, G. (2000). The marine osmium isotope record. *Terra Nova*,
806 12, 205-219.
- 807 Peucker-Ehrenbrink, B., & Ravizza, G. (2012). Osmium isotope stratigraphy. In *The Geologic*
808 *Time Scale*, 145-166.
- 809 Poag, C.W., Powars, D.S., Poppe, L.J., & Mixon, R.B. (1994). Meteoroid mayhem in Ole
810 Virginny: Source of the North American tektite strewn field. *Geology*, 22, 691-694.
- 811 Poirier, A., and Hillaire-Marcel, C. (2011). Improved Os-isotope stratigraphy of the Arctic
812 Ocean. *Geophysical Research Letters*, 38, L14607, doi:10.1029/2011GL047953.
- 813 Pollastro, R.M. & B. F. Bohor. 1993. Origin and clay-mineral genesis of the Cretaceous-Tertiary
814 boundary unit, Western Interior of North America. *Clays and Clay Minerals*, 41, 7-25.
- 815 Pospichal, J. J., & Wise, S.W. (1990), 37. Paleocene to Middle Eocene calcareous nannofossils of
816 ODP Sites 689 and 690, Maud Rise, Weddell Sea. *Proceedings of the Ocean Drilling*
817 *Program, Scientific Results*, 113, 613-638.
- 818 Premoli Silva, I., & Bolli, H. (1973), Late Cretaceous to Eocene planktonic foraminifera, and
819 stratigraphy of Leg 15, *Initial reports of the Deep Sea Drilling Project*, 15, 499-547.
- 820 Rampino, M. R., & Stothers, R. B. 1984. Terrestrial mass extinctions, cometary impacts and the
821 Sun's motion perpendicular to the galactic plane. *Nature*, 308, 709-712.
- 822 Raup, D. M., & Sepkoski, J. J. (1982). Mass extinctions in the marine fossil record. *Science*, 215,
823 1501-1503.
- 824 Ravizza, G., Blusztajn, J., & Prichard, H. M. (2001). Re–Os systematics and platinum-group
825 element distribution in metalliferous sediments from the Troodos ophiolite. *Earth and*
826 *Planetary Science Letters*, 188, 369-381.
- 827 Reimold, W.U., Ferrière, L., Deutsch, A., & Koeberl, C. (2014). Impact controversies: Impact
828 recognition criteria and related issues. *Meteoritics and Planetary Science*, 49, 723–731.
- 829 Renne, P.R., Deino, A.L., Hilgen, F.J., Kuiper, K.F., Mark, D.F., Mitchell, W.S., Morgan, L.E.,
830 Mundil, R., & Smit, J., 2013, Time scales of critical events around the Cretaceous-
831 Paleogene boundary: *Science*, 339, 684–687, <https://doi.org/10.1126/science.1230492>
- 832 Renne, P.R., Arenillas, I., Arz, J.A., Vajda, V., Gilabert, V. & Bermúdez, H.D. (2018). Multi-
833 proxy record of the Chicxulub impact at the Cretaceous-Paleogene boundary from
834 Gorgonilla Island, Colombia, *Geology*, 46, 547-550.

- 835 Riller, U., et al. (2018). Rock fluidization during peak ring formation of large impact craters,
836 *Nature*, 562, 511–518
- 837 Robin, E., Boclet, D., Bonte, P., Froget, L., Jehanno, C., & Rocchia, R. (1991). The stratigraphic
838 distribution of Ni-rich spinels in the Cretaceous-Tertiary boundary rocks at El Kef
839 (Tunisia), Caravaca (Spain) and 761C (Leg 122). *Earth and Planetary Science Letters*,
840 107, 715-721.
- 841 Robinson, N., Ravizza, G., Coccioni, R., Peucker-Ehrenbrink, B. & Norris, R., (2009). A high-
842 resolution marine $^{187}\text{Os}/^{188}\text{Os}$ record for the late Maastrichtian: Distinguishing the
843 chemical fingerprints of Deccan volcanism and the KP impact event. *Earth and Planetary
844 Science Letters*, 281, 159-168.
- 845 Rocchia, R., Boclet, D., Bonte, P., Froget, L., Galbrun, B., Jehanno, C. & Robin, E. (1992). Iridium
846 and other element distributions, mineralogy, and magnetostratigraphy near the Cretaceous/
847 Tertiary boundary in Hole 761C. *Proceedings of the Ocean Drilling Program, Scientific
848 Results*, 122, 753-762.
- 849 Rocchia, R., Robin, E., Froget, L., & Gayraud, J., (1996), Stratigraphic distribution of
850 extraterrestrial markers at the Cretaceous-Tertiary boundary in the Gulf of Mexico area:
851 Implications for the temporal complexity of the event, in G. Ryder, D. Fastovsky and S.
852 Gartner, eds., The Cretaceous-Tertiary boundary event and other catastrophes in earth
853 history, *Geological Society of America Special Paper 307*, Boulder, Colorado, 279–286.
- 854 Röhl, U., Ogg, J.G., Geib, T.L., & Wefer, G., (2001), Astronomical calibration of the Danian time
855 scale, *Geological Society, London, Special Publications*, 183, 163-183.
- 856 Romein, A. (1977), Calcareous nannofossils from Cretaceous-Tertiary boundary interval in
857 Barranco del Gredero (Caravaca, Prov-Murcia, SE Spain). *Proceedings of the Koninklijke
858 Nederlandse Akademie van Wetenschappen Series B-Palaeontology Geology Physics
859 Chemistry Anthropology*, 80, 256.
- 860 Sanford, J.C., Snedden, J.W., & Gulick, S.P. (2016), The Cretaceous-Paleogene boundary deposit
861 in the Gulf of Mexico: Large-scale oceanic basin response to the Chicxulub impact, *Journal
862 of Geophysical Research: Solid Earth*, 121, 1240-1261.
- 863 Schaller, M.F., Fung, M.K., Wright, J.D., Katz, M.E., & Kent, D.V. (2016), Impact ejecta at the
864 Paleocene-Eocene boundary, *Science* 354, 225-229.
- 865 Schueth, J. D., Bralower, T.J., Jiang, S., & Patzkowsky, M.E., (2015), The role of regional survivor
866 incumbency in the evolutionary recovery of calcareous nannoplankton from the
867 Cretaceous/Paleogene (K/Pg) mass extinction, *Paleobiology*, 41, 661-679.
- 868 Schulte, P., Deutsch, A., Salge, T., Berndt, J., Kontny, A., MacLeod, K.G., Neuser, R.D., &
869 Krumm S., (2009), A dual-layer Chicxulub ejecta sequence with shocked carbonates from
870 the Cretaceous–Paleogene (K–Pg) boundary, Demerara Rise, western Atlantic,
871 *Geochimica et Cosmochimica Acta*, 73, 1180-1204.
- 872 Schulte, P. et al., (2010), The Chicxulub asteroid impact and mass extinction at the Cretaceous-
873 Paleogene boundary, *Science*, 327, 1214-1218.
- 874 Schultz P.H. & D’Hondt S., (1996), Cretaceous-Tertiary (Chicxulub) impact angle and its
875 consequences, *Geology*, 24, 963-967.

- 876 Scotese, C.R., (2008). The PALEOMAP project PaleoAtlas for ArcGIS, Volume 2. Cretaceous
877 paleogeographic and plate reconstructions, PALEOMAP Project.
- 878 Shukolyukov, A. & Lugmair, G.W. (1998). Isotopic evidence for the Cretaceous-Tertiary impactor
879 and its type. *Science*, 282, 927-929.
- 880 Sigurdsson, H., D'Hondt, S., Arthur, M.A., Bralower, T.J., Zachos, J.C., van Fossen, M. and
881 Channel, J.E., (1991). Glass from the Cretaceous/Tertiary boundary in Haiti. *Nature*, 349
882 482.
- 883 Sigurdsson, H., Leckie, R.M., & Acton, G.D. (1997). Caribbean volcanism, Cretaceous/Tertiary
884 impact, and ocean climate history: synthesis of Leg 165. In *Proceedings of the Ocean*
885 *Drilling Program Initial Reports* 165, 377-402.
- 886 Smit, J. & J. Hertogen (1980). An extraterrestrial event at the Cretaceous-Tertiary boundary,
887 *Nature* 285: 198-200.
- 888 Smit, J. (1982), Extinction and evolution of planktonic foraminifera at the Cretaceous/Tertiary
889 boundary after a major impact, Geological implications of impacts of large asteroids and
890 comets on the Earth, *Geological Society of America Special Paper*, 190, 329-352.
- 891 Smit, J. & F.T. Kyte. (1984). Siderophile-rich magnetic spheroids from the Cretaceous-Tertiary
892 boundary in Umbria, Italy. *Nature*, 310, 403-405.
- 893 Smit, J. & Romein, A.J.T. (1985). A sequence of events across the Cretaceous-Tertiary boundary.
894 *Earth Planet. Sci. Lett.* 74:155-70
- 895 Smit J., Alvarez W., Montanari A., Swinburn N.H.M., Van Kempen T.M., Klaver G.T. and
896 Lustenhouwer W. J. (1992) "Tektites" and microkrystites at the Cretaceous-Tertiary
897 boundary: two strewn fields, one crater? *Lunar Planet. Sci.* 22, 87-100.
- 898 Smit, J. (1999), The global stratigraphy of the Cretaceous-Tertiary boundary impact ejecta, *Annual*
899 *Review of Earth and Planetary Sciences*, 27, 75-113.
- 900 Swisher, C.C., Grajales-Nishimura, J. M., Montanari, A., Margolis, S. V., Claeys, P., Alvarez, W.,
901 Renne, P., Cedillo-Pardo, E., Maurrasse, F. J-M. R., Curtis, G.H., Smit, J., & McWilliam,
902 M.O. (1992). Coeval $^{40}\text{Ar}/^{39}\text{Ar}$ ages of 65.0 million years ago from Chicxulub crater melt
903 rock and Cretaceous-Tertiary boundary tektites. *Science*, 257, 954-958.
- 904 Thierstein, H.R. (1982), Terminal Cretaceous plankton extinctions: A critical assessment, in
905 *Geological implications of impacts of large asteroids and comets on the earth*, 385-399.
- 906 Thierstein, H.R., & H. Okada (1979), The Cretaceous/Tertiary boundary event in the North
907 Atlantic, *Initial Reports of the Deep Sea Drilling Project*, 43, 601-616.
- 908 Thomas, E., & Monechi, S. (2007). Cenozoic mass extinctions in the deep sea: What perturbs the
909 largest habitat on Earth? *Geological Society of America Special Paper*, 424, 1-23.
- 910 Turekian, K.K., (1982). Potential of $^{187}\text{Os}/^{186}\text{Os}$ as a cosmic versus terrestrial indicator in high
911 iridium layers of sedimentary strata. In: Silver, L.T. & Schultz, P.H. (Eds.), Geological
912 Implications of Impacts of Large Asteroids and Comets on the Earth. *Geological Society*
913 *of America Special Paper* 190, 243-249.

- 914 Turgeon, S. C., & Creaser, R. A. (2008). Cretaceous oceanic anoxic event 2 triggered by a massive
915 magmatic episode. *Nature*, 454, 323.
- 916 Tyrrell, T., Merico, A., & McKay, D.I.A. (2015). Severity of ocean acidification following the
917 end-Cretaceous asteroid impact. *Proceedings of the National Academy of Sciences*, 112,
918 6556–6561. (doi:10.1073/pnas.1418604112)
- 919 Urrutia-Fucugauchi, J., Morgan, J., Stöffler, D., & Claeys, P. (2004). The Chicxulub Scientific
920 Drilling Project (CSDP). *Meteorit. Planet. Sci.*, 39, 787-790.
- 921 Westerhold, T., U. Röhl, I. Raffi, E. Fornaciari, S. Monechi, V. Reale, J. Bowles, & H. F. Evans
922 (2008), Astronomical calibration of the Paleocene time, *Palaeogeography,*
923 *Palaeoclimatology, Palaeoecology*, 257(4), 377-403.
- 924 Whalen, M.T., Gulick, S.P.S., Pearson, Z. F., Norris, R.D., Perez-Cruz, L., & Urrutia-Fucugauchi,
925 J. (2013). Annealing the Chicxulub impact: Paleogene Yucatán carbonate slope
926 development in the Chicxulub impact basin, Mexico. In, Deposits, Architecture, and
927 Controls of Carbonate Margin, Slope and Basinal Settings. *SEPM Special Publication* 105,
928 p. 282-304.
- 929 Vellekoop, J., Sluijs, A., Smit, J., Schouten, S., Weijers, J.W.H., Sinninghe Damsté, J.S., &
930 Brinkhuis, H., (2014). Rapid short-term cooling following the Chicxulub impact at the
931 Cretaceous–Paleogene boundary. *PNAS* 111, 7537-7541.
- 932 Zachos, J.C., Arthur, M.A., & Dean, W.E. (1989). Geochemical evidence for suppression of
933 pelagic marine productivity at the Cretaceous/Tertiary boundary. *Nature*, 337, 61-64.